

Roughness-enhanced transport in a tilted ratchet driven by Lévy noiseYongge Li,¹ Yong Xu,^{1,2,3,*} and Jürgen Kurths^{2,3}¹*Department of Applied Mathematics, Northwestern Polytechnical University, Xi'an 710072, China*²*Potsdam Institute for Climate Impact Research, 14412 Potsdam, Germany*³*Department of Physics, Humboldt University Berlin, 12489 Berlin, Germany*

(Received 21 August 2017; published 14 November 2017)

The enhanced transport of particles by roughness in a tilted rough ratchet potential subject to a Lévy noise is investigated in this paper. Due to the roughness, the transport process exhibits quite different properties compared to the smooth case. We find that the roughness on the potential wall functions like a ladder to provide the convenience for particles to climb up but hinder them to slide down. The mean first passage time from one well to its right adjacent well and the mean velocity are, respectively, calculated versus the roughness, the external force, and the Lévy stability index. Our results show that the roughness is able to induce an enhancement on the mean velocity of particles and accelerate the barrier crossing process. The general conditions require a small external force and a small Lévy stability index. We find that with increasing external forces, the enhancement areas of roughness and Lévy stability index both shrink. However, for the Lévy stability index within the enhancement area, its increase will enlarge the enhancement area of roughness. On the contrary, under the same conditions we observe that for a Gaussian noise the roughness always reduces the corresponding mean velocity which is very different from the case of Lévy noise.

DOI: [10.1103/PhysRevE.96.052121](https://doi.org/10.1103/PhysRevE.96.052121)**I. INTRODUCTION**

Energy landscapes are typically constructed to understand the spatial position distribution of particles and the corresponding potential energy level in systems of biology, chemistry, and physics, such as silicon nanocluster, protein folding, and spin glasses [1–3]. A common feature of such an energy landscape is its multimodalilty and metastability, and the distance of two adjacent stable points is large enough to gain a flat potential surface. However, in some specific cases the potential surface varies frequently with small potential wells within large potential wells, i.e., the system exhibits a rough energy landscape rather than a metastable one. A typical example in protein folding shows that the potential surface of a protein may exhibit a hierarchical structure containing a number of minima and maxima, which indicates that the underlying energy landscape is spatially rough due to multiple energy scales associated with the building blocks of proteins [4,5]. Besides the protein folding dynamics, a similar phenomenon has been found in other prominent systems such as activation gating of ion channels [6,7], diffusions in structural glasses [8,9], and supercooled liquids [10,11]. Motivated by the property of roughness, Zwanzig proposed to describe the rough potential by superimposing a fast oscillating trigonometric function onto the background potential function [12]. The amplitude of the trigonometric function is assumed to be small as a perturbation on the smooth background. This rough model provides an analytical tool to describe the properties of roughness. A typical application in biology is to measure the energy landscape roughness of proteins and RNA [13,14]. The deep and wide applications in various systems have motivated us to consider the exploration of properties of a rough potential.

Understanding the dynamical influences of roughness is one of the most challenging problems in related subjects.

However, the dynamics and theories induced by roughness are still quite close compared to the general smooth potential. In this seminal paper Zwanzig found that the roughness could reduce the effective diffusion coefficient as compared to the smooth potential [12]. Mondal showed that the superimposing of roughness decreases the current significantly for Gaussian noise [15]. Besides Zwanzig's rough model, another popular rough model is based on random or disordered potentials, whose roughness is dominated by the distribution of spatial noises. Relevant studies can be found in [16,17], and references therein. In this paper, however, we mainly consider Zwanzig's rough model.

Ratchet potential has applications in various fields such as molecular motors, optical lattices, quantum dot arrays, and pendulum motions [18–21] (and references therein). Besides the rich Brownian ratchet work, the Lévy ratchet has been analyzed and explored theoretically and numerically in many aspects, including the probability density function (PDF), barrier crossing, directional motion, and fractional Fokker-Planck equations [22–28]. As known, Lévy noise has a heavy tail of the probability density function and contains more large jumps than Gaussian noise. Various applications for Lévy noise have been found, in particular, in gene networks [29,30], neuron models [31], molecular motors [32], quantum dynamics [33], millennial climate changes [34], or insurance risks [35,36]. In addition, we have observed α -stable Lévy noise in laser gyroscope data with a stability index staying between 1.96 and 1.985 [37]. Recently, we investigated the dynamics of particles in a rough triple-well potential; interestingly, we found that the roughness helps particles to climb up the potential barriers [38]. Inspired by this, the mean velocity, splitting probability, and mean first passage time are analyzed in an asymmetric ratchet potential. The results show that with proper parameters, roughness is able to accelerate the transport of particles [39]. However, as mentioned above, the roughness leads to a reduction of the current in a Brownian ratchet [15]. Thus, the roughness does function differently with Lévy noise compared

*Corresponding author: hsux3@nwpu.edu.cn

to the Gaussian case. Then the combination of roughness and Lévy noise in a ratchet potential will induce various interesting phenomena. After superposition of roughness and the smooth tilted ratchet potential, we will demonstrate that the roughness has the ability to enhance the transport of particles in a tilted rough ratchet potential.

As the main quantitative characteristics in this paper, we will concentrate on the mean velocity (MV) and the mean first passage time (MFPT). The paper is organized as follows. In Sec. II, we introduce a tilted rough ratchet potential model excited by a Lévy noise. In Sec. III, we calculate MVs with respect to the roughness, the external force, and the Lévy index to examine enhancement effects of the superimposed roughness. In Sec. IV, the MFPTs as a function of the roughness under different Lévy parameters are explored. Finally, the conclusion is presented.

II. MODEL DESCRIPTION

We consider the motion of a particle in a periodic potential $U_0(x)$ subject to a constant external force F and Lévy noise $\dot{\xi}(t)$,

$$\gamma \dot{x} = -\frac{d}{dx}[U_0(x) - Fx] + \dot{\xi}(t). \quad (1)$$

Here, the overdot is the derivative with respect to time t . The friction coefficient γ can be omitted by rescaling the Langevin equation, thus for simplicity γ is assumed unity. $\dot{\xi}(t)$ is a symmetric α -stable Lévy motion, with its characteristic function

$$E[e^{ik\xi(t)}] = \exp[-tD|k|^\alpha], \quad (2)$$

where α [$\alpha \in (0, 2]$] is the stability index of the distribution describing the power-law tail of the PDF. D denotes the noise intensity. The formal derivative of $\dot{\xi}(t)$ is defined as Lévy noise. When $\alpha = 2.0$, the Lévy noise reduces to the Gaussian case.

The periodic potential is taken as $U_0(x) = -\cos(2\pi\omega_0x)$, and ω_0 is the frequency, thus the period is $L = 1/\omega_0$. To get a rough potential, we superimpose a rapidly oscillating trigonometric function $U_1(x)$ on the background potential $U_0(x)$. $U_1(x)$ can be regarded as a perturbation on the relative slowly varying $U_0(x)$. The superimposed perturbed function $U_1(x)$ is defined as

$$U_1(x) = \varepsilon \sin(\omega_1x), \quad \varepsilon \ll 1.0, \quad (3)$$

where ε is the amplitude of the roughness which is assumed to be far below 1.0. ω_1 determines the frequency of the roughness which is required to be $\omega_0 \ll \omega_1$ to ensure that $U_1(x)$ oscillates rapidly. Typically we assume $\omega_1 = 100$ and $\omega_0 = 1$ in this work. The superposition of $U_0(x)$ and $U_1(x)$ leads to a rough ratchet potential with multiple small wells. By coupling with the external force F , we obtain the new Langevin equation as

$$\dot{x} = -\frac{d}{dx}U_{\text{eff}}(x) + \dot{\xi}(t), \quad (4)$$

$$U_{\text{eff}}(x) = -Fx - \cos(2\pi x) + \varepsilon \sin(100x),$$

in which $U_{\text{eff}}(x)$ is the effective tilted rough ratchet potential. An illustration of $U_{\text{eff}}(x)$ is shown in Fig. 1. In the absence

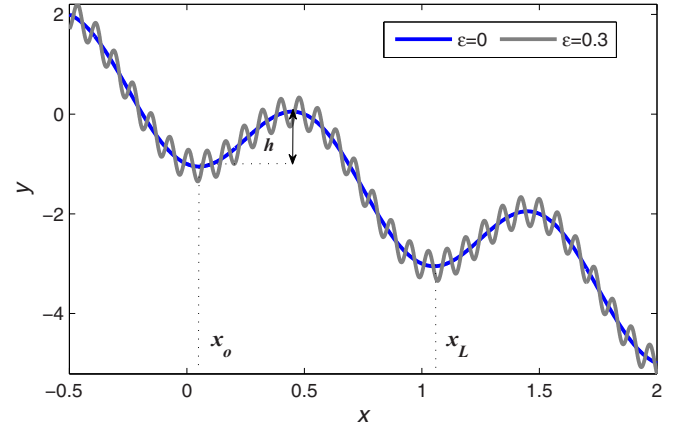


FIG. 1. An illustration of the effective rough potential $U_{\text{eff}}(x)$ in Eq. (3). The period length of $U_0(x)$ is taken as $L = 1.0$, and the external force $F = 2.0$. The two labeled stable points of $U_0(x) - Fx$ are $x_0 = \arcsin(F/2\pi)/2\pi$ and $x_L = L + x_0$.

of roughness, the stable points of the tilted ratchet locate at $x_{nL} = nL + \arcsin(F/2\pi)/2\pi$; n is an integer. F affects the steepness and locations of stable points. To ensure that $U_0(x) - Fx$ has stable points, we restrict $F < 2\pi$ and in this paper we only consider the case $F > 0$. The superposition of roughness introduces a number of small wells on the tilted ratchet potential which look like ladders on the potential walls. The larger the ω_1 the denser the ladderlike wells. In addition, with increasing ε the small wells become deeper, making it much easier to trap particles or slow down the transport.

In a tilted ratchet potential, there are several ways to accelerate the transport of particles, such as increasing the external force F , enlarging the noise intensity D , and lowering the barrier height h [18,40,41]. For a Lévy noise, it is additionally possible to get a faster MV with a smaller Lévy stability index α [25]. However, we find that the superimposed roughness on the tilted ratchet potential is able to enhance the transport in a different regime under Lévy noises. Next, we will analyze how roughness induces an enhancement effect based on the MV and MFPT versus F , α , and ε , respectively.

III. ENHANCEMENT EFFECT ON THE MV

The first basic quantity of this paper is the MV of a particle in the tilted rough ratchet potential subject to a Lévy noise. Under the condition of Gaussian noises, the MV or probability current has been investigated both theoretically and numerically in various studies. In most situations, the explicit analytical formula of MV can be obtained by solving the Fokker-Planck equation (FPE). However, for systems subjected to a Lévy noise, the corresponding FPE equation becomes of fractional order, for which it is very difficult to obtain an analytical solution. Up to now, only systems with specific polynomial potentials have been solved analytically [42,43]. Numerically simulating the fractional-order FPE is an important way to deal with this problem. However, for a periodic potential the precision depends sensitively on the integration domain, boundary conditions, and the external

force [27,44]. So in this tilted rough ratchet potential, we directly calculate Eq. (3) with the Euler algorithm. Considering the influences of roughness, the mean displacement of a one-step iteration must be far smaller than the period length of $U_1(x)$. This requires a very small time step. In this paper, the time step is $\Delta t = 10^{-4}$. To calculate the MV, the process is repeated more than 10^4 times for each point and the total integration time is not less than 5×10^6 . The MV is calculated by

$$v = \langle \dot{x} \rangle = \lim_{t \rightarrow \infty} \frac{\langle x(t) - x(0) \rangle}{t}, \quad (5)$$

where $\langle x(t) - x(0) \rangle$ is the statistical mean (first moment) of the particle displacements as a function of time. For Lévy noise, when $\alpha \in (1, 2]$ the first moment is finite, whereas it is divergent for $\alpha \in (0, 1)$. Hence, we mainly focus on the influences of $\alpha \in (1, 2]$.

Figures 2(a) and 2(b) show the MVs as a function of F for different roughness ε . As known, a driving force $F \neq 0$ will break the symmetry and generates a tilted potential. Thus a net current yields a biased direction. As expected, MVs increase monotonously with F in both panels. However, after the superposition of roughness, the transport properties become complex. In Fig. 2(a), with increasing F , the roughness first leads to an increase of the MV, but then it decreases. This phenomenon indicates that the roughness can result in an enhancement of the transport. Due to the fact that small wells on the walls service as stopovers for particles to temporarily stay, particles are able to jump to right-side wells from somewhere uphill with a small F . However, for a large F , when roughness is absent, particles may be able to slide down the smooth ratchet directly, or at least it is easy for them to cross barriers. When the roughness is superimposed, small rough wells on the potential make it impossible for particles to slide down directly like in the smooth case. The roughness may even become an obstacle to be overcome. Thus the roughness hinders the transport of particles in a steep tilted ratchet rather than helps it. Besides F , a comparison of Figs. 2(a) and 2(b) implies that the Lévy index α is also an important factor to affect the influence of roughness. When $\alpha = 2.0$, no matter how F varies, the roughness always reduces the transport velocity. This is because Gaussian noises have no large jumps to kick particles out of a potential well with one large excitation like Lévy noises (with small α). This makes small rough wells bad barriers rather than helpful ladders. Coupled with the mentioned influences of F , the hindering effect is reasonably obvious for large F when $\alpha = 2.0$ [Fig. 2(b)].

The enhancement areas of ε accelerating the transport in the direction of F are briefly shown in Figs. 2(c) and 2(d) for different F . In Fig. 2(c), MVs first increase and then decrease for different F . This phenomenon indicates that there always exists an optimal ε to maximize the MV. Increasing F , the locations of the optimal ε shift to the left, i.e., for large F particles take more advantage of small roughness, while for small F particles benefit more from large roughness. The enhancement areas of the aggressive ε narrow gradually with increasing F . When $\alpha = 1.9$ for $F \leq 2.0$, MVs increase with the roughness, i.e., all ε shown in the panel enhance the transport. However, when $F \geq 3.0$, the roughness hinders the transport suddenly even for very small ε . Hence, a large

external force F will shrink the enhancement area of ε , while a small F accelerates the transport. To obtain a view of the continuous changes of MV with respect to F and ε , Fig. 2(e) is plotted, in which the inset shows clearly that the enhancement area of ε decreases with increasing F . In Fig. 2(f), the vertical view of $v_\varepsilon - v_{\varepsilon=0}$ demonstrates the strength of enhancement and suppression, where the optimal ε lies in the dark red area, and the most suppressing ε is within the blue area.

In summary, we find that a proper ε is able to enhance the transport. The basic conditions require a small F and an α away from 2.0. Next, we will discuss the dependence of the enhancement area on the Lévy noise index, α .

The shaded parts in Fig. 3 are enhancement areas, i.e., the roughness is capable of increasing MVs in the ratchet. In these shaded areas, we always find an aggressive ε to enhance the transport. In Fig. 3 we calculate MVs with the minimal roughness index $\varepsilon = 0.1$. There is no doubt that for some $\varepsilon < 0.1$ the roughness may also increase MVs, so the enhancement area is not exactly precise. But it is certain that the parameters in the shaded area will definitely enhance the transport. In our simulated results, with increasing F , we find that the enhancement area shrinks for larger α . The white parts in Fig. 3 mainly focus on large α . This is due to the fact that larger α generate fewer and smaller jumps, which makes it less possible for particles to make use of the roughness as for smaller α . In particular, for large ε the roughness has high potential barriers, i.e., particles are easily trapped in these small wells for a while which delays the transport. Note that, although in Figs. 3(c) and 3(d) the shown roughness reduces MVs slightly for small α , the roughness does enhance the transport with an even smaller $\varepsilon < 0.1$. The insets in both figures show that each of two cases has a small enhancement area of ε . However, this is not true for large α ; for example, when $F = 4.0$ the MV of $\alpha = 1.8$ decreases monotonously with increasing ε [see Fig. 4(b)]. The bifurcation diagram of α and F is computed in Fig. 3(e) where the gray color is the enhancement area labeled under the condition of $v_{\varepsilon=0.05} - v_{\varepsilon=0} > 0$, and the white color is the suppressing area labeled for the condition of $v_{\varepsilon=0.05} - v_{\varepsilon=0} < 0$. It shows that with increasing F , the enhancement area shrinks and the suppressing area of α focuses at the right side.

Figure 4 illustrates the dependence of enhancement effects on ε for different values of α . It clearly shows the enhancement areas of ε accelerating the transport. MVs first increase with ε but then decrease for $\alpha \leq 1.8$. This means that for these α , we can find an optimal ε to maximize the MVs. In addition, the locations of the optimal ε shift to the right with the increase of α . For example, the enhancement area of the aggressive ε for $\alpha = 1.5$ is about $(0, 0.19]$, and we get the maximal MV at about $\varepsilon = 0.1$. However, when $\alpha = 2.0$ the enhancement area disappears, which coincides with the conclusion in [15]. In Fig. 4(a), the enhancement areas of ε increase with α , but it comes to a sudden change at around $\alpha = 1.93$, i.e., the range of the aggressive ε vanishes for $1.93 < \alpha \leq 2.0$. In Fig. 4(b) we see that a large F not only shrinks the enhancement area of α , but also reduces the range of the aggressive ε . When $F = 4.0$, the range of the aggressive ε is about $(0, 0.13]$ for $\alpha = 1.5$, which is much smaller than that of $F = 2.0$. These phenomena are clearly illustrated in Fig. 4(c) and the changes of the optimal ε can be found in Fig. 4(d).

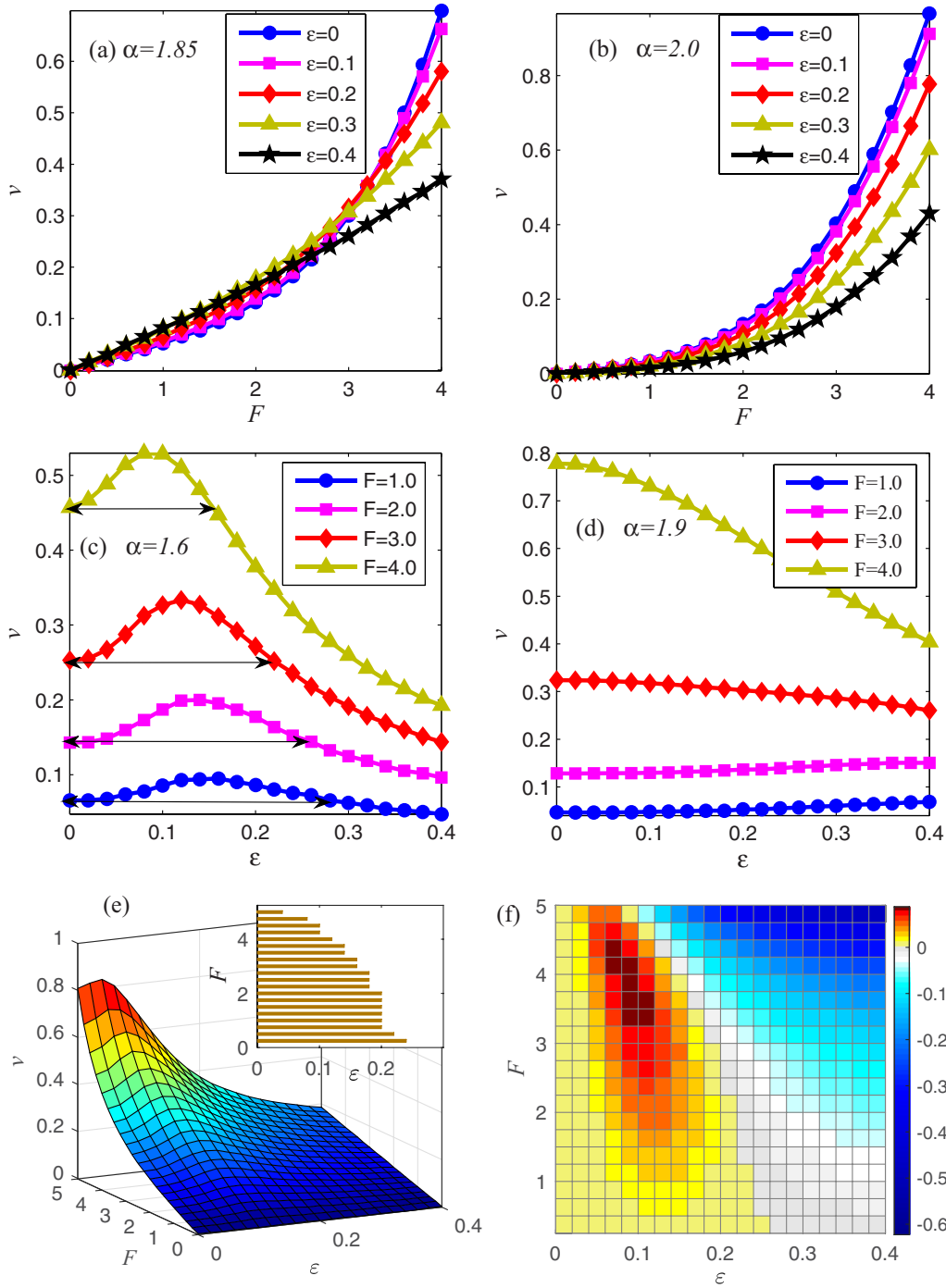


FIG. 2. MVs with respect to the external force F and roughness ε for different α , with $D = 0.3$. (a) $\alpha = 1.85$; roughness can increase the MV for small F . (b) $\alpha = 2.0$; roughness always decreases the MV. (c) $\alpha = 1.6$; the enhancement areas of ε shrink with increasing F . (d) $\alpha = 1.9$; the influence of ε suddenly changes from enhancement to suppression with increasing F . (e) The space diagram of MV for $\alpha = 1.5$. The inset shows the enhancement area of ε , in which the difference $\Delta\varepsilon = 0.02$ makes the changes of bar unsmooth. (f) is the vertical view of $v_\varepsilon - v_{\varepsilon=0}$, where we can find the enhancement area and optimal ε for different F . The legend in (a) and (b) for ε holds throughout the paper.

From these MVs we find that a proper ε is able to enhance the transport in the direction of F for α away from 2.0. For $\alpha = 2.0$, the enhancement effect vanishes for all ε , no matter how F varies. The increase of F not only shrinks the enhancement area of α , but also reduces the range of the aggressive ε . A small F and a modest α will probably induce an enhancement effect on the transport velocity.

IV. ENHANCEMENT EFFECT ON THE MFPT

In this section, we analyze the MFPT problem under the condition of roughness. The MFPT describes how long a particle jumps from one area to another specific region. When $\alpha = 2.0$ in a tilted periodic potential, the MFPT can be given in a simple form closely related to the MV,

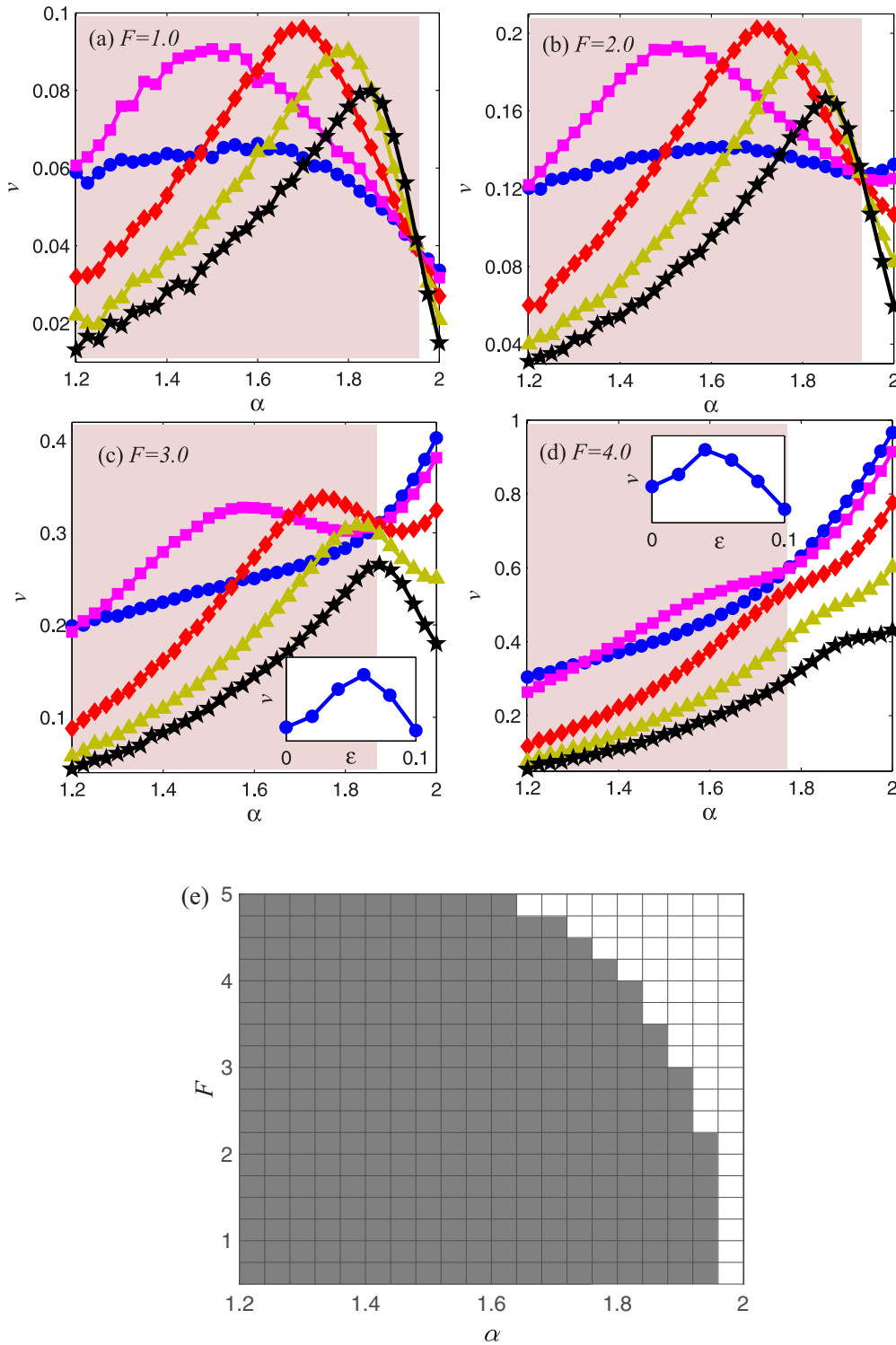


FIG. 3. MVs as a function of α for different F with $D = 0.3$. The shaded parts are enhancement areas of α in which roughness increases MVs. The enhancement areas shrink with increasing F . The insets in (c) and (d) are plotted to illustrate that small α is within the enhancement areas for some $\epsilon < 0.1$. (e) The bifurcation diagram of α and F , in which the gray color corresponds to the enhancement area, and the white is the suppressing area.

$v = L / \langle t(x_0 \rightarrow x_L) \rangle$, where $\langle t(x_0 \rightarrow x_L) \rangle$ is the MFPT from x_0 to x_L [26]. However, this does not fit for Lévy noise. This is because Gaussian noise has almost no large jumps; most of the time a particle can only cross one well once. So each time a particle jumps out, it is probably not beyond x_{nL} , $n \geq 2$.

However, for a Lévy noise, when a particle jumps out, it can be far from x_L . Thus the formula works for Gaussian noise, but for Lévy noise the formula is not applicable. Here we investigate how roughness affects the MFPT from x_0 to x_L , considering a particle starting from the initial point x_0

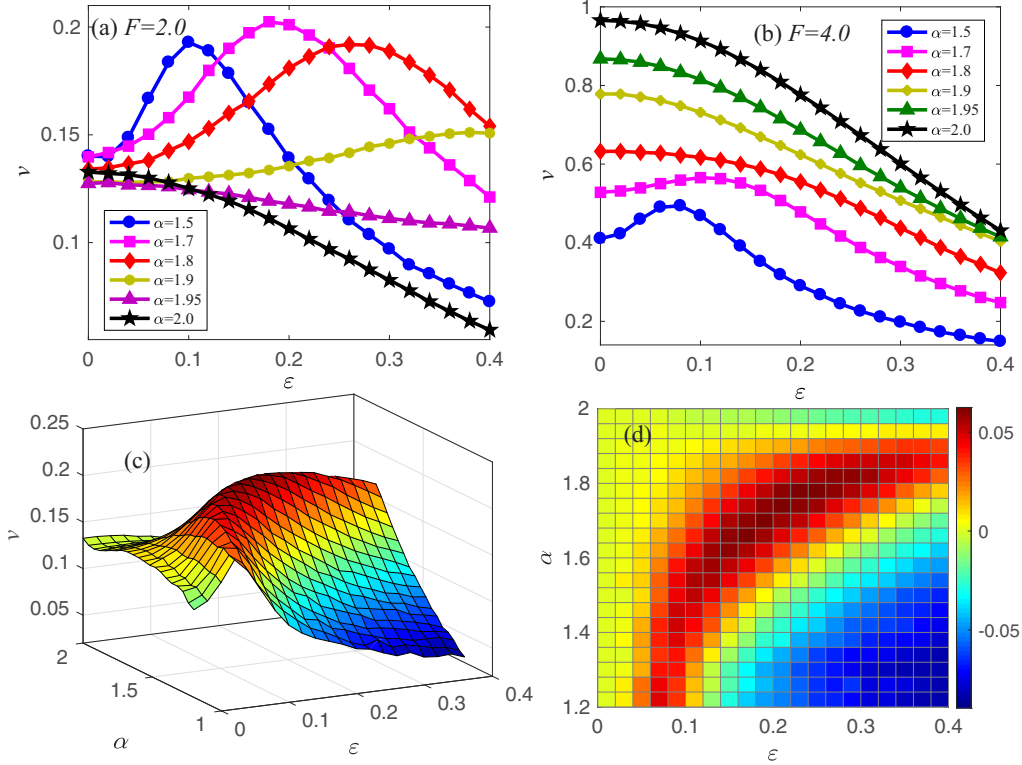


FIG. 4. (a), (b) MVs as a function of ϵ for different α with $D = 0.3$ in cases $F = 2.0$ and $F = 4.0$. With increasing α , the enhancement areas of ϵ increase for small α , but then encounter a sudden change from enhancement to suppression. (c) The space diagram of MV with respect to ϵ and α for $F = 2.0$. (d) The vertical view of $v_\epsilon - v_{\epsilon=0}$, from which we can find the variation of optimal ϵ .

and proceeding until it arrives or crosses the right adjacent stable point x_L . The corresponding MFPT is defined as follows:

$$\text{MFPT} = \langle \inf\{t : x(t) \geq x_L \mid x(0) = x_0\} \rangle. \quad (6)$$

As expected, the external force F leads to a reduction of the MFPT. This corresponds to MVs shown in Fig. 2, i.e., larger F lead to faster MVs. When the roughness is superimposed in Fig. 5(a), with increasing F , the roughness induces a decrease of MFPT first, and then increases the MFPT. But

for α close to 2.0, it is hard for the roughness to reduce the MFPT. We see that the roughness no longer accelerates the crossing for $\alpha = 1.98$. As mentioned above, the roughness always decreases the MV in the Gaussian case, thus with the relation $\langle v \rangle = L / \langle t(x_0 \rightarrow x_L) \rangle$, we know the roughness will certainly increase the MFPT.

Figure 6 illustrates the influences of roughness on the MFPT with respect to α for different F . In the absence of roughness, for $F = 1.0$ the MFPT first decreases slightly but then increases fast. However, for $F = 2.0$ and $F = 3.0$ MFPTs

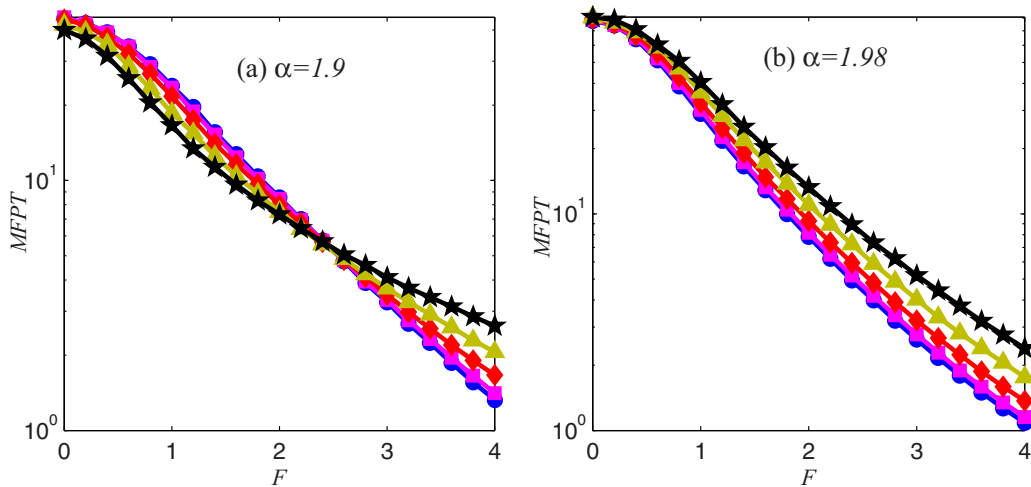


FIG. 5. MFPTs with respect to F with $D = 0.3$. For $\alpha = 1.9$ the roughness can decrease the MFPT for small F ; however, for $\alpha = 1.98$ the roughness always increases the MFPT.

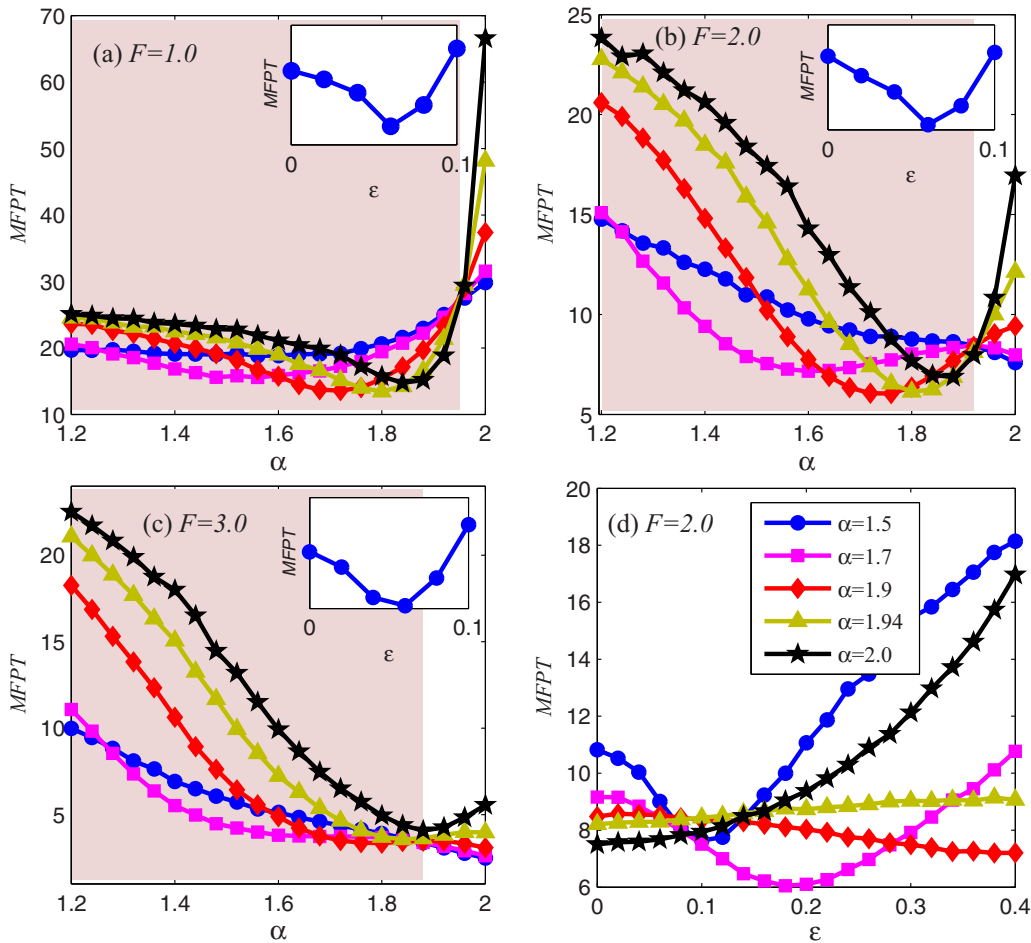


FIG. 6. MFPTs with respect to α and ϵ with $D = 0.3$. With increasing F , the enhancement areas of α shrink. The insets in (a)–(c) illustrate that $\alpha = 1.2$ decreases MFPTs for some $\epsilon < 0.1$. (d) shows the influences of ϵ for different α .

decrease monotonously with α , i.e., when F is large the jumps hinder the right crossing process and lead to a longer MFPT than α of less jumps. This is because when F is large the tilted ratchet is steep, and it is easy for a particle to go down with even small fluctuations. However, when we add large jumps,

particles may be kicked to a far place in the negative direction by a big excitation. This will force particles to move a long way to come back and move to x_L . On the other hand, large jumps and modest jumps have small differences on crossing a small positive distance L . Then a small α does not have

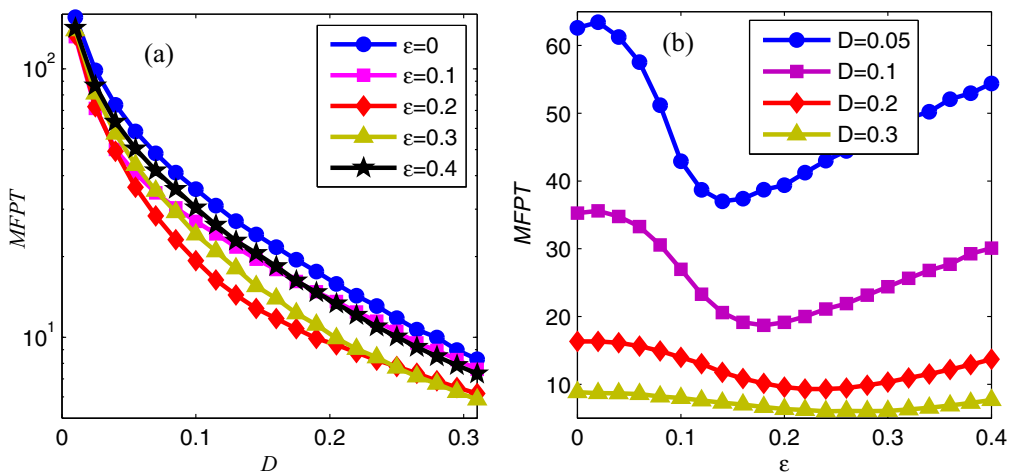


FIG. 7. MFPTs with respect to D and ϵ , for $\alpha = 1.8$, $F = 2.0$.

much advantage on the MFPT, although it has a lot of large jumps. Therefore, small fluctuations are relatively helpful on the MFPT for large F .

When the roughness is superimposed, MFPTs show a remarkable increase for α close to 2.0. Although the roughness $\varepsilon = 0.1$ increases the MFPT slightly for small α like $\alpha = 1.2$ in Figs. 6(a)–6(c), $\varepsilon < 0.1$ does reduce the MFPT (see the inset). Thus for small α and ε , the roughness leads to an acceleration of the crossing process. Figure 6(d) shows the evolution of the MFPT with respect to ε in detail for different α with $F = 2.0$. As shown, for small α the MFPT first decreases but then increases, i.e., there is an optimal ε to let a particle cross beyond x_L with minimal time. But for large α , the roughness may increase or decrease the MFPT monotonously like $\alpha = 1.9$ and $\alpha = 1.94$, respectively.

Another important parameter in the study of MFPT is the noise intensity. Choosing a set of parameters $\alpha = 1.8$ and $F = 2.0$ in Fig. 7, the MFPT reduces with increasing noise intensity D . The roughness always accelerates the crossing process, which coincides with Fig. 6(b). In Fig. 7(b), MFPTs first decrease and then increase, and the variation rate between maximum and minimum is larger for small D . In addition, the optimal ε inducing the minimal MFPT shifts to the right with the increase of D . This means that a small noise intensity benefits more from the small roughness, while a large noise intensity benefits more from the large roughness.

V. CONCLUSION

In this paper, we have studied the enhanced transport resulting from the superimposed roughness in a tilted rough ratchet potential subject to a Lévy noise. The mean velocity and mean first passage time have been calculated to explore the enhancement areas with respect to the driving force F , the Lévy stability index α , and the noise intensity D under

perturbations of roughness. We find that the superposition of roughness is able to accelerate the transport of particles with a proper F and α . For the mean velocity, the enhancement area of ε decreases, and the optimal ε shifts to the left with increasing F for small α . For large α , the enhancement area of ε exhibits a sudden change from a full range to a zero range with increasing F . We conclude that a large F benefits more from a small ε , whereas a small F benefits more from a large ε . In addition, the enhancement area of α decreases with increasing F and focuses at regions away from $\alpha = 2.0$. Within the enhancement area of α , the increasing of α leads to a larger range of aggressive ε , and shifts the optimal ε to the right. This phenomenon indicates that a small α benefits more from a small ε while a large α benefits more from a large ε . The results of our investigations of the mean first passage time almost coincide with those of the mean velocity. The roughness can accelerate the crossing process with a small force for α away from 2.0. Moreover, we find that the roughness functions strongly for small noise intensities, i.e., the induced rate of change of MFPTs is larger for smaller noise intensities. In summary, the roughness is able to enhance the transport of particles in a tilted rough ratchet in specific conditions requiring a small F and α away from 2.0. However, except the above parameters, other factors influencing the function of roughness are its frequency or forms, which will be discussed in our future work.

ACKNOWLEDGMENTS

This work was supported by the NSF (China) 11772255, the Fundamental Research Funds for the Central Universities, Innovation Foundation for doctor dissertation, and Top International University Visiting Program for Outstanding Young scholars of NPU. Y.X. thanks the Alexander von Humboldt Foundation (Germany) for support.

-
- [1] D. J. Wales, *Energy Landscapes: Applications to Clusters, Biomolecules and Glasses* (Cambridge University Press, Cambridge, 2004).
 - [2] *Rugged Free Energy Landscapes: Common Computational Approaches to Spin Glasses, Structural Glasses and Biological Macromolecules*, edited by W. Janke (Springer, Berlin, Heidelberg, 2008).
 - [3] H. Yu, D. R. Dee, X. Liu, A. M. Brigley, I. Sosova, and M. T. Woodside, *Proc. Natl. Acad. Sci. USA* **112**, 8308 (2015).
 - [4] H. Frauenfelder, S. G. Sligar, and P. G. Wolynes, *Science* **254**, 1598 (1991).
 - [5] A. Ansari, J. Berendzen, S. F. Bowne, H. Frauenfelder, I. E. Iben, T. B. Sauke, E. Shyamsunder, and R. D. Young, *Proc. Natl. Acad. Sci. USA* **82**, 5000 (1985).
 - [6] L. Delemotte, M. A. Kasimova, M. L. Klein, M. Tarek, and V. Carnevale, *Proc. Natl. Acad. Sci. USA* **112**, 124 (2015).
 - [7] T. Linder, B. L. de Groot, and A. Stary-Weinzinger, *PLoS Comput. Biol.* **9**, e1003058 (2013).
 - [8] P. Charbonneau, J. Kurchan, G. Parisi, P. Urbani, and F. Zamponi, *Nat. Commun.* **5**, 3725 (2014).
 - [9] J. C. Ye, J. Lu, C. T. Liu, Q. Wang, and Y. Yang, *Nat. Mater.* **9**, 619 (2010).
 - [10] A. Heuer, B. Doliwa, and A. Saksengwitt, *Phys. Rev. E* **72**, 021503 (2005).
 - [11] P. G. Debenedetti and F. H. Stillinger, *Nature (London)* **410**, 259 (2001).
 - [12] R. Zwanzig, *Proc. Natl. Acad. Sci. USA* **85**, 2029 (1987).
 - [13] C. Hyeon and D. Thirumalai, *Proc. Natl. Acad. Sci. USA* **100**, 10249 (2003).
 - [14] R. Nevo, V. Brumfeld, R. Kapon, P. Hinterdorfer, and Z. Reich, *EMBO Rep.* **6**, 482 (2005).
 - [15] D. Mondal, P. K. Ghosh, and D. S. Ray, *J. Chem. Phys.* **130**, 074703 (2009).
 - [16] F. Marchesoni, *Phys. Rev. E* **56**, 2492 (1997).
 - [17] S. Banerjee, R. Biswas, K. Seki, and B. Bagchi, *J. Chem. Phys.* **141**, 124105 (2014).
 - [18] P. Reimann, *Phys. Rep.* **361**, 57 (2002).
 - [19] P. Reimann, C. Van den Broeck, H. Linke, P. Hänggi, J. M. Rubi, and A. Pérez-Madrid, *Phys. Rev. Lett.* **87**, 010602 (2001).
 - [20] P. Hänggi and F. Marchesoni, *Rev. Mod. Phys.* **81**, 387 (2009).
 - [21] Y. G. Li, Y. Xu, W. Xu, Z. C. Deng, and J. Kurths, *Phys. Rev. E* **96**, 022152 (2017).
 - [22] I. Pavlyukevich, Y. G. Li, Y. Xu, and A. V. Chechkin, *J. Phys. A: Math. Theor.* **48**, 495004 (2015).

- [23] I. Pavlyukevich, B. Dybiec, A. V. Chechkin, and I. M. Sokolov, *Eur. Phys. J.: Spec. Top.* **191**, 223 (2010).
- [24] B. Dybiec, *Phys. Rev. E* **78**, 061120 (2008).
- [25] D. del-Castillo-Negrete, V. Yu. Gonchar, and A. V. Chechkin, *Physica A* **387**, 6693 (2008).
- [26] B. Dybiec, E. Gudowska-Nowak, and I. M. Sokolov, *Phys. Rev. E* **78**, 011117 (2008).
- [27] A. Kullberg and D. del-Castillo-Negrete, *J. Phys. A: Math. Theor.* **45**, 255101 (2012).
- [28] Y. Xu, H. Li, H. Y. Wang, W. T. Jia, X. L. Yue, and J. Kurths, *J. Appl. Mech.* **84**, 091004 (2017).
- [29] J. Wu, Y. Xu, H. Y. Wang, and J. Kurths, *Chaos* **27**, 063105 (2017).
- [30] Y. Xu, Y. G. Li, H. Zhang, X. F. Li, and J. Kurths, *Sci. Rep.* **6**, 31505 (2016).
- [31] Z. Q. Wang, Y. Xu, and H. Yang, *Sci. China-Technol. Sci.* **59**, 371 (2016).
- [32] B. Lisowski, D. Valenti, B. Spagnolo, M. Bier, and E. Gudowska-Nowak, *Phys. Rev. E* **91**, 042713 (2015).
- [33] G. G. Carlo, G. Benenti, G. Casati, and D. L. Shepelyansky, *Phys. Rev. Lett.* **94**, 164101 (2005).
- [34] P. D. Ditlevsen, *Geophys. Res. Lett.* **26**, 1441 (1999).
- [35] K. C. Yuen and C. C. Yin, *Math. Comput. Model.* **53**, 1700 (2011).
- [36] C. C. Yin, Y. Z. Wen, and Y. X. Zhao, *ASTIN Bull.* **44**, 635 (2014).
- [37] X. R. Shen, H. Zhang, Y. Xu, and S. X. Meng, *IEEE Sens. J.* **16**, 1998 (2016).
- [38] Y. G. Li, Y. Xu, J. Kurths, and X. L. Yue, *Phys. Rev. E* **94**, 042222 (2016).
- [39] Y. G. Li, Y. Xu, J. Kurths, and X. L. Yue, *Chaos* **27**, 103102 (2017).
- [40] M. Gitterman and V. Berdichevsky, *Phys. Rev. E* **65**, 011104 (2001).
- [41] P. Reimann, C. Van den Broeck, H. Linke, P. Hänggi, J. M. Rubi, and A. Pérez-Madrid, *Phys. Rev. E* **65**, 031104 (2002).
- [42] A. Chechkin, V. Gonchar, J. Klafter, R. Metzler, and L. Tanatarov, *Chem. Phys.* **284**, 233 (2002).
- [43] A. A. Dubkov, B. Spagnolo, and V. V. Uchaikin, *Int. J. Bifurc. Chaos Appl. Sci. Eng.* **18**, 2649 (2008).
- [44] S. A. Ibáñez, A. B. Kolton, S. Risau-Gusman, and S. Bouzat, *J. Stat. Mech.* (2011) P08025.